Joint Performance in Bonded Concrete Overlays of Asphalt

John DeSantis, Julie Vandenbossche, Kevin Alland, Steven Sachs, Thomas Burnham, and Aldo Montenegro

Abstract

Bonded concrete overlays of asphalt pavements (BCOA), also known as whitetopping, consist of a thin concrete overlay on distressed asphalt or composite pavements. They typically have smaller panel sizes than traditional jointed plain concrete pavements (JPCP) in order to reduce stress levels. Faulting at the transverse joints is a distress in BCOA that is not currently addressed in current design procedures. The pumping mechanism that leads to this distress is the focus of this paper. Pumping in BCOA can develop at either the bottom of the overlay slab within the asphalt layer or at the bottom of the asphalt in the granular layer. It is essential to identify where the faulting initiates for each pavement structure, if accurate faulting models are to be developed for these pavement structures. An examination was conducted of 21 BCOAs located at the Minnesota Road Research Facility (MnROAD) to investigate how faulting initiates in BCOA and the rate at which it develops. To do this, the relationship between deflection load transfer efficiency (LTE) from falling weight deflectometer (FWD) testing and transverse joint faulting was examined. It was found that these parameters can be used in successfully defining when faulting initiates at the top of the asphalt and when it initiates at the top of the granular layer below the asphalt. Finally, the rate of the development of faulting in BCOAs resulting from pumping at the concrete/asphalt interface as well as pumping below the asphalt layer was compared to faulting predictions using current models. A good agreement between the observed and predicted faulting was not achieved.

Introduction

Bonded concrete overlays of asphalt pavements (BCOA), also known as whitetopping, consist of a new Portland cement concrete (PCC) overlay placed on an existing distressed asphalt or composite pavement. This rehabilitation technique is intended as a cost effective solution for marginally distressed in-service asphalt pavements. The existing asphalt is often milled prior to overlay construction to remove any surface distress and to increase the surface area to promote greater bond between the PCC and asphalt. These structures typically have smaller panel sizes than traditional jointed plain concrete pavements (JPCP) to reduce curling and warping stresses and bending stresses produced by applied loads (Mack et al. 1993; Mack et al. 1998; Wu et al. 1998). In BCOA, the existing asphalt layer assists in carrying a portion of the load.

Problem Statement

Faulting in BCOA, like other PCC surfaced pavements, is caused by the pumping mechanism. To date, faulting is not considered in the design process for BCOA. Before faulting can be incorporated into the design process, a better understanding of where it initiates and how it develops must be achieved. Pumping in BCOA can develop at either the bottom of the overlay slab within the asphalt layer or below the asphalt in the granular layer. If the transverse joint in the overlay does not activate through the asphalt layer then pumping of the asphalt material occurs at the top of the asphalt layer, as shown in Figure 1a. If the transverse joint activates through the asphalt layer, then the PCC and asphalt act as a monolithic structure and faulting develops due to pumping of the granular material below the asphalt, as shown in Figure 1b. Voids beneath the slab can also develop due to break down of the asphalt layer, as shown in Figure 1c (Rasmussen et al. 2002). However, while these voids will likely result in the development of longitudinal cracks in the wheelpath, or diagonal cracks originating at the intersection of the wheelpath and transverse joint at the bottom of the slab, they do not contribute to faulting and therefore will not be discussed.

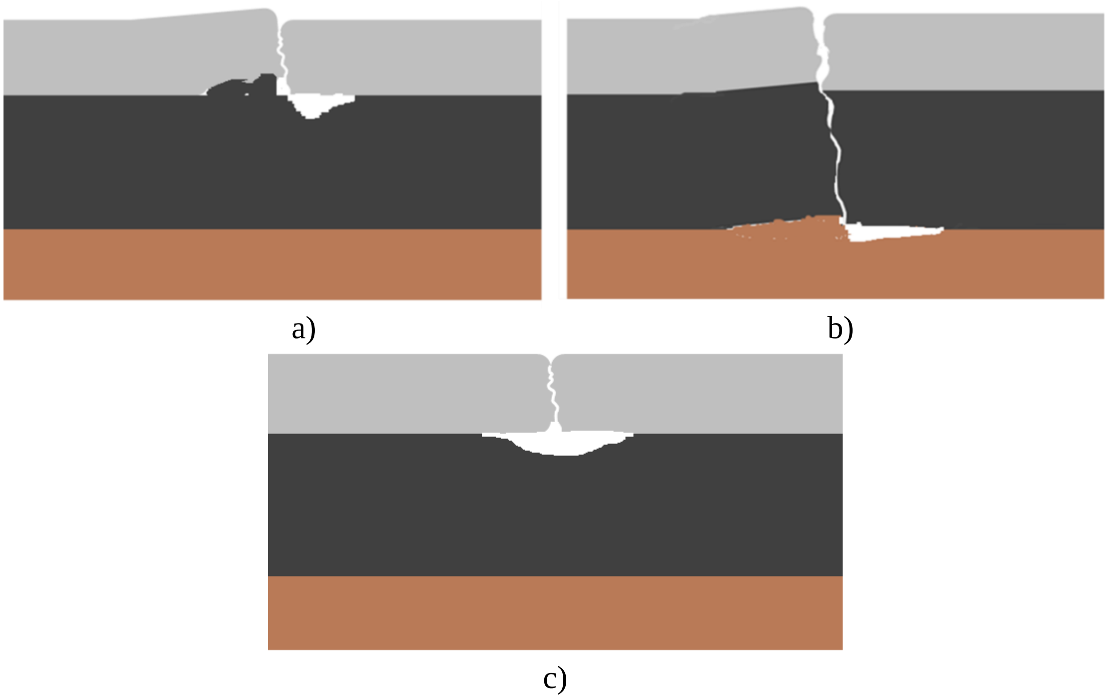

Figure 1 Joint Propagation: a) Pumping of the Asphalt, b) Pumping of the Granular Material, and c) Deterioration of the Asphalt

Scope of Work

There are three main objectives of this study. The first objective is to use the extensive falling weight deflectometer (FWD) data and distress data available at the Minnesota Road Research Facility (MnROAD) to identify which joints at the test facility activate through the asphalt. The deflection load transfer efficiency (LTE) of a joint can be used to identify if a crack has fully activated through the asphalt layer (Roesler et al. 2008). The measured LTE at a fully activated joint will be lower than at a joint that has not activated through the asphalt. Differential deflections as well as the maximum deflections also provide useful information in interpreting the depth of crack activation. Cores at the joint are taken to validate the methods of classifying joint activation using the FWD data.

The second objective is to determine if the depth of crack propagation can be established based on critical design features without the availability of extensive FWD data. Once the depth of activation is established using FWD data under the first objective, the combination of the critical design features contributing to crack activation through the asphalt layer can be identified.

The third objective is to investigate the rate at which faulting develops over time in BCOA. Specifically, it is important to determine if the shape of the faulting development curve is similar whether pumping is occurring at the PCC/asphalt interface, or at the top of the granular layer directly below the asphalt. The suitability of the faulting prediction model in the Pavement ME design procedure to predict this curve is then investigated.

Depth of Joint Activation

FWD data was examined for all the BCOAs constructed at MnROAD to identify the depth of joint activation. The 21 sections examined as part of this study are part of the mainline test section that experiences live interstate traffic diverted from I-94. The design features for each test section have been provided in Table 1. All of the test sections were placed on an existing hot mix asphalt pavement that was constructed in 1993 on a silty-clay subgrade. The existing pavement was milled to the thicknesses shown in Table 1 prior to construction of the overlay. This removed any surface distresses and increased the surface area for bonding between the overlay and asphalt layer. None of these sections have edge drains. The mainline is subjected to approximately 1 million 80-kN (18-kips) ESALs per year. Cells 60 through 63 were subjected to 6.74 million equivalent single axle loads (ESALs) over 6.6 years (Li and Vandenbossche 2013).

Table 1 BCOA Cells at MnROAD

Cell	Panel Size LxW m (ft)	Dowels mm (in)	Transverse Joint Sealant	PCC Thickness mm (in)	Asphalt Thickness mm (in)	Year Constructed	Year Removed	Shoulder	Fibers	Cell Length m (ft)
60	1.5x1.8 (5x6)	No	Yes	127 (5)	178 (7)	2004	2013	Asphalt	None	69 (225)
61	1.5x1.8 (5x6)	No	No	127 (5)	178 (7)	2004	2013	Asphalt	None	69 (225)
62	1.5x1.8 (5x6)	No	Yes	102 (4)	203 (8)	2004	2013	Asphalt	None	69 (225)
63 [1]	1.5x1.8 (5x6)	No	No	102 (4)	203 (8)	2004	2013	Asphalt	None	69 (225)
92	3x3.7 (10x12)	25.4 (1)	Yes	152 (6)	178 (7)	1997	2010	Asphalt	Polypropylene	55 (180)
93	1.2x1.2 (4x4)	No	Yes	102 (4)	229 (9)	1997	2004	Asphalt	Polypropylene	91 (300)
94	1.2x1.2 (4x4)	No	Yes	76 (3)	254 (10)	1997	2004	Asphalt	Polypropylene	91 (300)
95	1.5x1.8 (5x6)	No	Yes	76 (3)	254 (10)	1997	2004	Asphalt	Polyolefin	91 (300)
96 [1]	1.5x1.8 (5x6)	No	Yes	152 (6)	178 (7)	1997	-	Asphalt	Polyolefin	55 (180)
97	3x3.7 (10x12)	No	Yes	152 (6)	178 (7)	1997	2010	Asphalt	Polypropylene	49 (160)
114	1.8x1.8 (6x6)	25.4 (1)	No	152 (6)	127 (5)	2008	-	Asphalt	None	30 (99)
214	1.8x1.8 (6x6)	No	No	152 (6)	127 (5)	2008	-	Asphalt	None	7 (24)
314	1.8x1.8 (6x6)	25.4 (1)	No	152 (6)	152 (6)	2008	-	Asphalt	None	42 (138)
414	1.8x1.8 (6x6)	No	No	152 (6)	152 (6)	2008	-	Asphalt	None	9 (30)
514	1.8x1.8 (6x6)	25.4 (1)	No	152 (6)	178 (7)	2008	-	Asphalt	None	11 (36)
614	3.7x1.8 (12x6)	Flat Plate	No	152 (6)	178 (7)	2008	-	Asphalt	None	33 (108)
714	1.8x1.8 (6x6)	25.4 (1)	No	152 (6)	191 (7.5)	2008	-	Asphalt	None	5 (18)
814	1.8x1.8 (6x6)	No	No	152 (6)	203 (8)	2008	-	Asphalt	None	7 (24)
914	1.8x1.8 (6x6)	25.4 (1)	No	152 (6)	203 (8)	2008	-	Asphalt	None	24 (78)
160	1.8x1.8 (6x6)	No	Yes	127 (5)	152 (6)	2013	-	Asphalt	Fibermesh 650	135 (444)
162	1.8x1.8 (6x6)	No	Yes	102 (4)	178 (7)	2013	-	Asphalt	Fibermesh 650	141 (462)

[1] 6.35 mm (0.25 in) of diamond grinding was performed on September 8, 2011

(http://dotapp7.dot.state.mn.us/research/dataproduct/Data%20Release/)

The FWD data collected in the outer wheelpath of the driving lane was used to determine the LTE, differential deflection between the loaded and unloaded side of the joint and the maximum measured deflection at the center of the load plate. First the LTE was used to determine if the cracks at the transverse joints had fully activated through the PCC and asphalt layers, as shown in Figure 1b. In BCOA, when the asphalt is continuous and uncracked it will contribute significantly more to LTE than if a crack is present. The LTE was measured on both the approach and leave side of the joint and was defined using the following equation:

$$LTE = \frac{\Delta_{UL}}{\Delta_L} * 100 \qquad \text{Equation (1)}$$

where Δ_{UL} is the deflection of the unloaded slab, and Δ_L is the deflection of the loaded slab. The minimum LTE between the approach and leave LTE was used. FWD testing was conducted at four joints in each of Cells 60, 61, 62, and 63 throughout their service lives and half of the total joints were tested before being taken out of service. Testing was conducted at the four joints per cell at a minimum of twice a year. Cells 93, 94, and 95 were tested at two joints, each at a minimum of twice a year. Cells 92, 96 and 97 were tested at two joints, each over the first four years. After this, testing was increased to approximately 10 joints per cell. One to three joints per cell were tested in Cells 114 through 914 (these cells were primarily used for verification). If the LTE of a joint was very low (below 50%) or much lower (more than 20% lower) than the LTE of a typical joint in the cell, then the joint was considered to propagate through the asphalt.

Two joints in Cell 96 (152-mm (6-in) thick) that exhibited transverse joint faulting were examined to validate the method for determining the depth of activation at the joint based on LTE. It was believed based on the LTE data that faulting at these joints was occurring due to pumping at different depths within the BCOA. The LTE at Joint B (Joint 2241) is also about 20 percent less than at Joint A (Joint 2236), which is a good indication that this joint has cracked through the asphalt. Faulting and LTE data can be seen in Figure 2. Faulting measurements six years after construction indicate Joints A and B had similar magnitudes of faulting, as shown in Figure 2. This cell was diamond ground to restore ride after 14 years in-service. When a pavement is diamond ground, only the surface distress is removed. Therefore, it is expected that faulting trends would continue after grinding. However, comparing these two joints four years after grinding, the fault depth at Joint B is 2 mm (0.08 in) greater than Joint A. This could be attributed to the fact that the pumping mechanism continues to transfer the base material and the fault depth continued to increase at Joint B. However, it is difficult to establish the faulting that developed at these joints due to the lack of measurements between 2003 and 2014. Cores were taken recently at these joints to validate the findings. As predicted, Joint B exhibited a crack through the asphalt, similar to the joint shown in Figure 1b, whereas Joint A did not. Joint A is more representative of the joint shown in Figure 1a. These cores can be seen in Figure 3. Note the condition of the asphalt directly below the concrete.

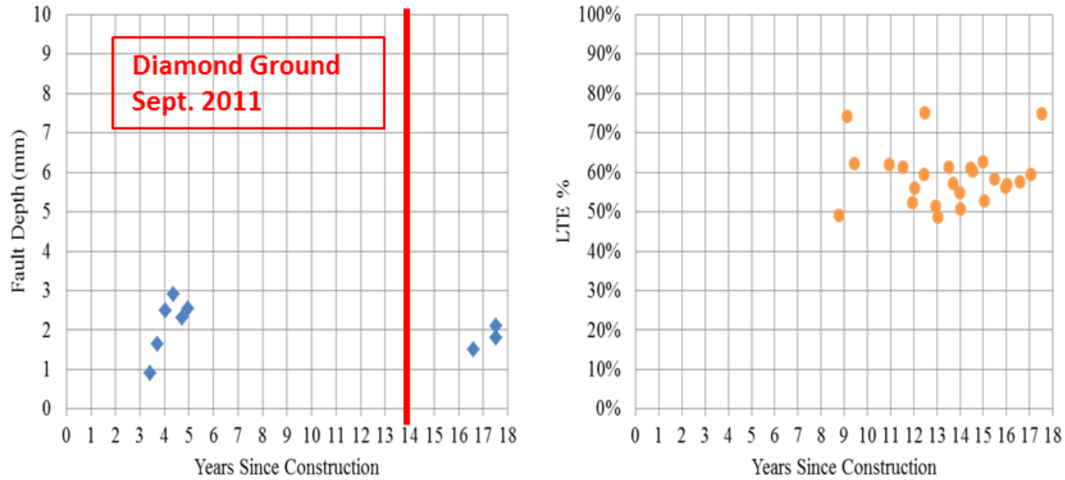

a) Joint A: Crack through PCC Only

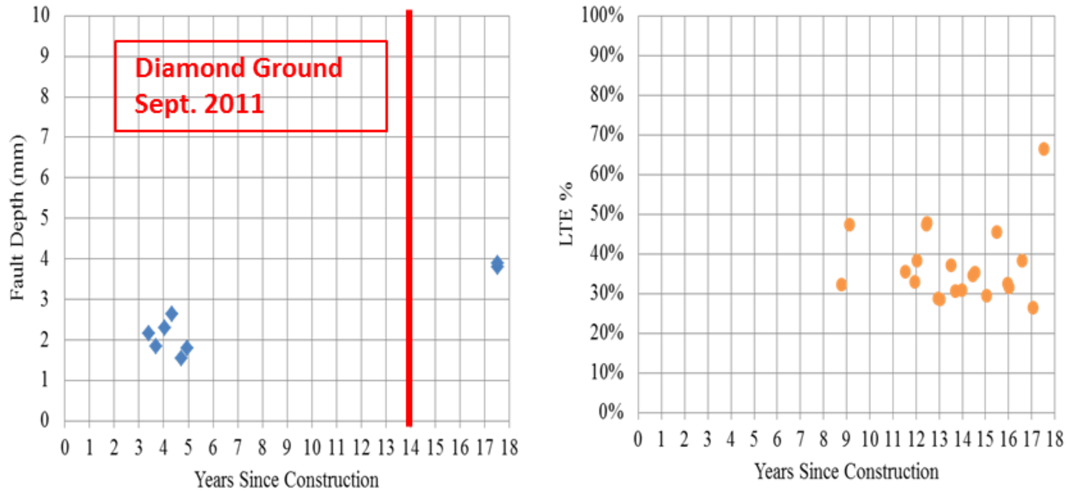

b) Joint B: Crack through PCC and Asphalt

Figure 2 Faulting and LTE for Joints in Cell 96

a) Joint A b) Joint B

Figure 3 Cell 96 Field Cores

Table 2 presents whether full depth activation through the asphalt is expected out of the total number of joints tested for each MnROAD cell for different criteria. Based on the LTE from this analysis, it appears that cracks propagated through the asphalt for all of the joints in the large undoweled panels of Cell 97. Cracks propagated through the asphalt for at least some of the joints in Cells 60, 61, and 96, and the cracks did not appear to propagate through the asphalt for Cells 62, 63, 93, 94, and 95. Cell 92 was inconclusive based upon LTE because the joints contained dowel bars and maintained a high LTE of 70 percent at all of the joints.

Table 2 Full Depth Activation

	Full Depth Activation Based on:		
Cell	LTE	Differential Deflections	Maximum Deflections
60	1/4	1/4	1/4
61	1/4	1/4	2/4
62	0/4	0/4	0/4
63	0/4	0/4	0/4
92	Inconclusive		
93	0/2	0/2	0/2
94	0/2	0/2	0/2
95	0/2	0/2	0/2
96	4/9	3/9	3/9
97	10/10	10/10	10/10

Another parameter examined was the deflections in the outer wheelpath under the 40-kN (9-kip) FWD load. Differential deflections are required for pumping to occur in PCC pavements. The same deflections used to calculate the LTE were used to determine the differential deflection across a joint. The following equation was used:

$$Differential\ Deflection = \Delta_L - \Delta_{UL} \qquad \text{Equation (2)}$$

where Δ_L is the maximum deflection of the loaded slab, and $\Delta_{UL}$is the maximum deflection of the unloaded slab. The maximum differential deflection between testing on the approach and leave slab was used in the analysis. Figure 4a shows the differential deflections for Joint A (discussed previously), and Figure 4b shows the differential deflections for Joint B. It can be seen that the differential deflections and the maximum deflections are both higher and more scattered when the crack propagates through the asphalt.

For Cells 93, 94, 95 and 97, the initial differential deflections over the first few years in-service remained between 0 and 0.025 mm (0 and 0.001 in) for a 40-kN (9-kip) load. The differential deflections were between 0 and 0.05 mm (0 and 0.002 in) for Cells 60 through 63 and 96 over the first few years in-service. If the joint exhibited an increase in differential deflections that was greater than 0.15 mm (0.006 in) and exhibited some variability, similar to Figure 4b, it indicates the joint most likely cracked through the asphalt. This variability, or scatter, is similar to what is seen in traditional JPCP and may be due to the discontinuity in the asphalt allowing the adjacent slabs to curl freely with changing temperature gradients. When minimal or no differential deflections are present, then it is likely that the joint did not crack through the asphalt. The cells in which at least some of the joints activated can be seen in Table 2. The results of the determination of the joints with full depth activation based upon differential deflections is identical to what was found by evaluating LTE.

The maximum deflection measured at the center of the load plate was also examined as a potential indicator of the depth at which the crack propagated, as can be seen in Figure 4. When this deflection was greater than 0.3 mm (0.012 in) for a 40-kN (9-kip) load it appears the joints cracked through the asphalt. It should be remembered that this criteria, as well as the criteria above, was established based on the subgrades and materials used at MnROAD and might not be representative of other BCOA. From Table 2, the results of the determination of full depth activation based upon maximum deflection are identical to the determination from LTE.

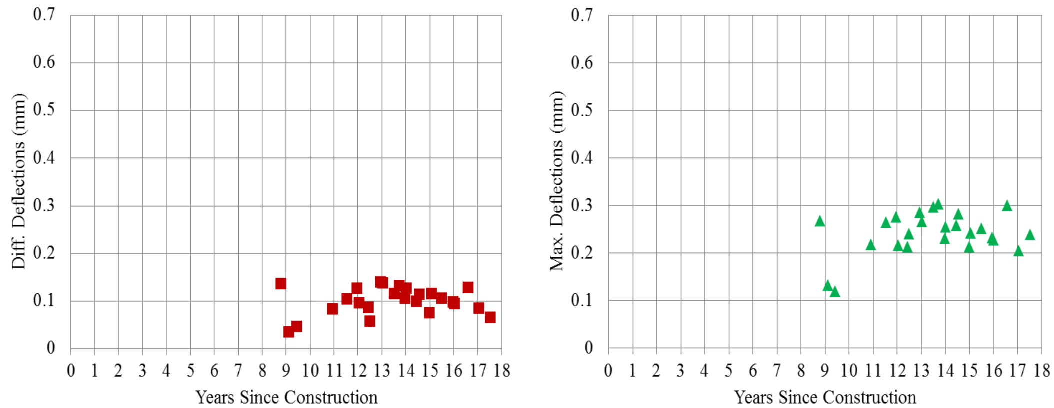

a) Joint A: Crack through PCC Only

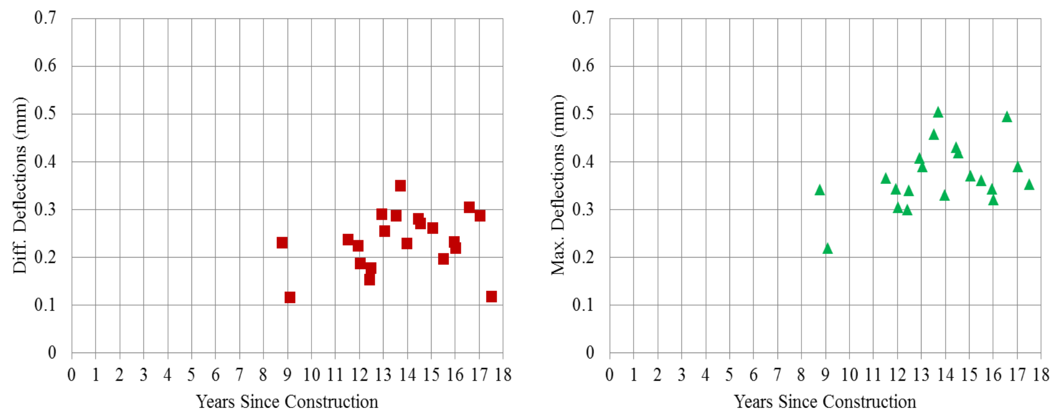

b) Joint B: Crack through PCC and Asphalt

Figure 4 Deflections under 40-kN (9-kip) Load

Factors Affecting Depth of Joint Activation

Joint activation in BCOA is a complicated process involving the coupling of the structural properties, material properties, and environmental conditions experienced by the BCOA. Critical stresses in the asphalt layer at the joint are likely a combination of Mode 1 (direct tension) and Mode 2 (shear) stresses. When the overlay experiences uniform volume reduction due to a temperature decrease or drying shrinkage, the continuous asphalt layer restrains the shrinkage. If the viscoelastic and fracture properties of the asphalt do not allow for the layer to absorb the strain without fracturing, the asphalt will fail in a Mode 1 fracture activating the joint through the asphalt. This stress is critical in the winter when the stiffness of the asphalt is highest, the maximum allowable strain in the asphalt is lowest, and the contraction of the concrete overlay is the highest. The asphalt also exhibits shear stress along the joint due to wheel loads. These stresses would be critical in the summer months when the asphalt stiffness is at a minimum. This critical stress, however, occurs when LTE due to aggregate interlock would be highest. Therefore, the joint activation mechanism is most likely dominated by Mode 1 fracture.

The mechanism of joint activation is similar in many ways to the propagation of reflective temperature cracks into the PCC overlay from the existing asphalt layer. This cracking was previously studied at MnROAD using the same BCOA sections. It was determined that the most influential variable in predicting if reflective cracking would propagate up from the asphalt into the overlay was the flexural stiffness ratio (FSR) between the PCC and asphalt layers. The flexural stiffness of each layer can be calculated using Equation 3 (Vandenbossche and Fagerness 2002). It was shown that temperature cracks in the asphalt would reflect up into the overlay if the FSR was less than 1.

$$Flexural\ Stiffness = D_i = \frac{E_i h_i^3}{12(1-\mu_i^2)} \qquad \text{Equation (3)}$$

$$FSR = \frac{D_{PCC}}{D_{Asphalt}} \qquad \text{Equation (4)}$$

where D is the flexural stiffness of layer i, E is the elastic modulus of layer i, h is the thickness of layer i, and μ is the Poisson's ratio of layer i. This was found to also be a critical value for determining whether joints activate through the asphalt layer.

Based on the joint activation mechanisms previously described, panel size is also likely to influence joint activation. Smaller panels result in less accumulated strain occurring at each joint, reducing the total stress in the asphalt at the joints. Material properties such as the coefficient of thermal expansion of the PCC and asphalt, ultimate drying shrinkage of the PCC, creep compliance of the asphalt, and fracture properties of the PCC and asphalt also can influence whether cracks activate through the asphalt. The effect of panel size is also a function of the environmental conditions. Environmental strains in the overlay can develop relatively rapidly, such as through a daily temperature cycle. The magnitude of the strain in the asphalt is then a function of the magnitude of the daily temperature swings and the panel size. Environmental strains can also develop more slowly, due to seasonal temperature changes or long term drying shrinkage. While these can be larger in magnitude as compared to the daily cycles in temperature, the slower development time provides a greater opportunity for the strains in the asphalt to dissipate through creep. Of course the magnitude of these strains are a function of both the yearly climatic conditions as well as the panel size.

Based on the discussion presented above, the design features of the cells at MnROAD were evaluated to determine if the depth of crack activation could be established based on several critical design features. To begin, the FSR for the cells at MnROAD representing conditions during the summer and winter months were calculated and are provided in Table 3. The stiffness of the asphalt was obtained based on a relationship established between the resilient modulus measured from cores taken from these cells and temperature (Vandenbossche and Fagerness 2002). The asphalt stiffness in the summer is based on an asphalt temperature of 38℃ (100℉) and a temperature of -16℃ (4℉) in the winter, which were measured using thermocouples. The material properties of the PCC for Cells 60 through 63 were provided by Burnham (Burnham 2006). The material properties of the PCC for Cells 93 through 97 and further information about these cells has been summarized as well elsewhere (Vandenbossche and Rettner 1999; Vandenbossche and Fagerness 2002; Burnham 2005). Using this information and the analysis performed under objective 1, the BCOAs that exhibited an average FSR less than or equal to 0.4 in the winter months were determined to be unlikely to develop a crack through the asphalt layer. A BCOA with a ratio greater than or equal to 0.9 in the winter months are likely to develop a crack through the asphalt layer. No conclusions could be made at this time on structures with ratios in between this range. Unfortunately, at MnROAD the panel size is confounded with FSR, so it is difficult to determine whether panel size influenced the activation of joints through the asphalt. Additionally, all of the materials used in the BCOA cells at MnROAD have similar material properties and are exposed to the same environmental conditions making it difficult to quantify the effect of these factors on joint activation.

It is interesting to note that in Cells 62, 63, 93, 94, and 95 the joints did not activate through the asphalt but thermal cracks did reflect up into the PCC overlay (Vandenbossche and Barman 2010). It can also be noted that Cells 60, 92, 96, and 97 showed that the joints activated through the asphalt but these cells did not exhibit reflective thermal cracking (Vandenbossche and Barman 2010). Cell 61, which is the same design as Cell 60 but with unsealed joints, exhibited joint activation through the asphalt and also was identified as having thermal cracks reflect up into the PCC overlay.

Table 3 Pavement Design Features Influencing Full Depth Joint Activation

Cell	Panel Size LxW m (ft)	PCC Elastic Modulus MPa (ksi)	Asphalt Elastic Modulus		PCC Poisson's Ratio	Asphalt Poisson's Ratio	FSR (Summer)	FSR (Winter)	Full-Depth Joint Activation (FSR/FWD)
			Summer MPa (ksi)	Winter MPa (ksi)					
60	1.5x1.8 (5x6)	32000 (4600)	1200 (170)	11000 (1600)	0.18	0.35	9.0	1.0	(Yes/Some)
61	1.5x1.8 (5x6)	30000 (4400)	1200 (170)	11000 (1600)	0.18[1]	0.35	8.7	0.9	(Yes/Some)
62	1.5x1.8 (5x6)	34000 (4900)	1200 (170)	11000 (1600)	0.18[1]	0.35	3.3	0.4	(No/None)
63	1.5x1.8 (5x6)	34000 (5000)	1200 (170)	11000 (1600)	0.18[1]	0.35	3.4	0.4	(No/None)
92	3x3.7 (10x12)	33000 (4800)	1200 (170)	11000 (1600)	0.2	0.35	16.4	1.8	(Yes/Unknown)
93	1.2x1.2 (4x4)	33000 (4800)	1200 (170)	11000 (1600)	0.19	0.35	2.3	0.2	(No/None)
94	1.2x1.2 (4x4)	33000 (4800)	1200 (170)	11000 (1600)	0.18	0.35	0.7	0.1	(No/None)
95	1.5x1.8 (5x6)	30000 (4400)	1200 (170)	11000 (1600)	0.19	0.35	0.6	0.1	(No/None)
96	1.5x1.8 (5x6)	33000 (4800)	1200 (170)	11000 (1600)	0.2	0.35	16.4	1.8	(Yes/Some)
97	3x3.7 (10x12)	33000 (4800)	1200 (170)	11000 (1600)	0.2	0.35	16.4	1.8	(Yes/All)

[1]Poisson’s Ratio reported for these cells are unreasonably low, typical values were assumed.

Trends in Development of Faulting

Pumping and faulting can occur whether or not the joint activates all the way through the asphalt layer. Staining along the shoulder, typically seen as an indicator of pumping, occurs at MnROAD in locations where the joint activates through the asphalt, as well as in joints that just activate through the concrete layer. Figure 5 shows the shoulders at a joint in Cell 61, which likely activated through the asphalt, and a joint in Cell 63, which likely did not activate through the asphalt. In both cases the shoulders show evidence of pumping. It is also important to note that the shoulders at MnROAD are not full depth. The observed signs of pumping may be due to lane shoulder pumping.

a) Cell 61: FSR_{Winter}=0.9, PCC = 127 mm (5 in), Asphalt = 178 mm (7 in)

b) Cell 63: FSR_{Winter}=0.4, PCC = 102 mm (4 in), Asphalt = 203 mm (8 in)

Figure 5 Evidence of Pumping at MnROAD

The rate of faulting and the shape of the faulting development curve vary based on several factors, including whether the joint activates through the asphalt, panel size, and joint sealant. Transverse joint faulting measurements were taken, on average, twice per year at approximately half of the joints in Cells 60 through 63 and at every joint in Cells 92 through 97, 114 through 914, 160, and 162. Although measurements were taken in both wheelpaths in both the driving and passing lane, this study focuses on the faulting measurements taken in outside wheelpath of the driving lane.

When the FSR_{winter} of the section was low (below 0.4), very little faulting occurred in the first few years, followed by a rapid increase in fault depth. An example of this faulting development can be seen in Figure 6a. When a BCOA has a low FSR, the pumping mechanism occurs at the interface between the PCC and asphalt layers. Early in the life of the pavement the bond between the PCC and asphalt is intact. This prevents water from penetrating the PCC/asphalt interface, thereby minimizing the pumping mechanism during the first few years. When this bond deteriorates, water can penetrate this interface. Since the asphalt layer has very little permeability, this water can be effectively trapped and lead to the rapid development of stripping and faulting at the PCC/asphalt interface.

When the FSR_{winter} of the section is high (above 0.9), little faulting is observed in the first few years, followed by a gradual development of faulting, with the rate of the development of faulting decreasing with time. Examples of this faulting pattern can be seen in Figures 7b and 7c. The initial low rate of faulting is likely caused by two factors. First, it may take time for the crack at the joint to propagate completely through the asphalt layer. Therefore, asphalt continuity may be conserved for the first few years of the service life, limiting differential deflections. Also, the sections are primarily undoweled. Load transfer through aggregate interlock is highest early in the service life. Therefore, differential deflections will be lower in this time frame.

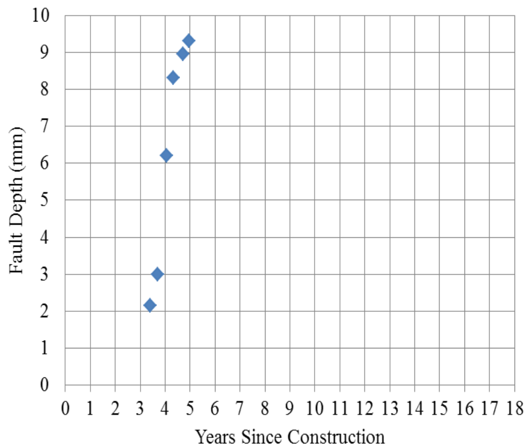

a) Cell 93, FSR= 0.2
1.2 by 1.2 m (4 by 4 ft)

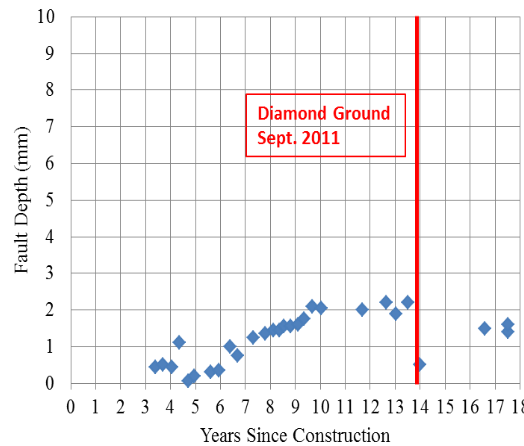

b) Cell 96, FSR = 1.8
1.5 by 1.8 m (5 by 6 ft)

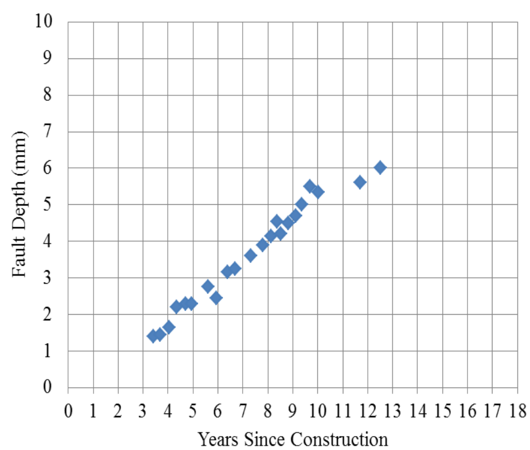

c) Cell 97, FSR = 1.8
3 by 3.7 m (10 by 12 ft)

Figure 6 Faulting Development of MnROAD BCOA Based on Panel Sizes

Panel size may also influence fault development. Larger panel sizes will have wider joints. This likely accelerated the development of faulting. Cell 96 and 97, which are shown in Figure 6b and 6c, have similar designs. Only the panel size varies. The joints shown in the figures likely both activated through the asphalt layer, however Cell 97 experienced significantly more faulting.

When the joint does not activate through the asphalt, sealing of the joints can have a large influence on the development of faulting. Water is required for the pumping mechanism to occur. If the joint does not activate through the asphalt, the only way for water to enter the joint is through the pavement surface. The asphalt layer has very low permeability, so once water enters the joint, it can become trapped, and cause rapid development of faulting. This makes sealing the joints more critical for BCOA with low FSR than for other PCC pavement structures. The structure of Cells 62 and 63 are identical, however, Cell 62 has sealed joints and Cell 63 does not. Cell 63 developed significantly more faulting than Cell 62. The faulting depths of the joints along the two cells can be seen in Figure 7. Also note, these measurements were taken right before being taken out of service and Cell 63 was diamond ground two years prior to these measurements.

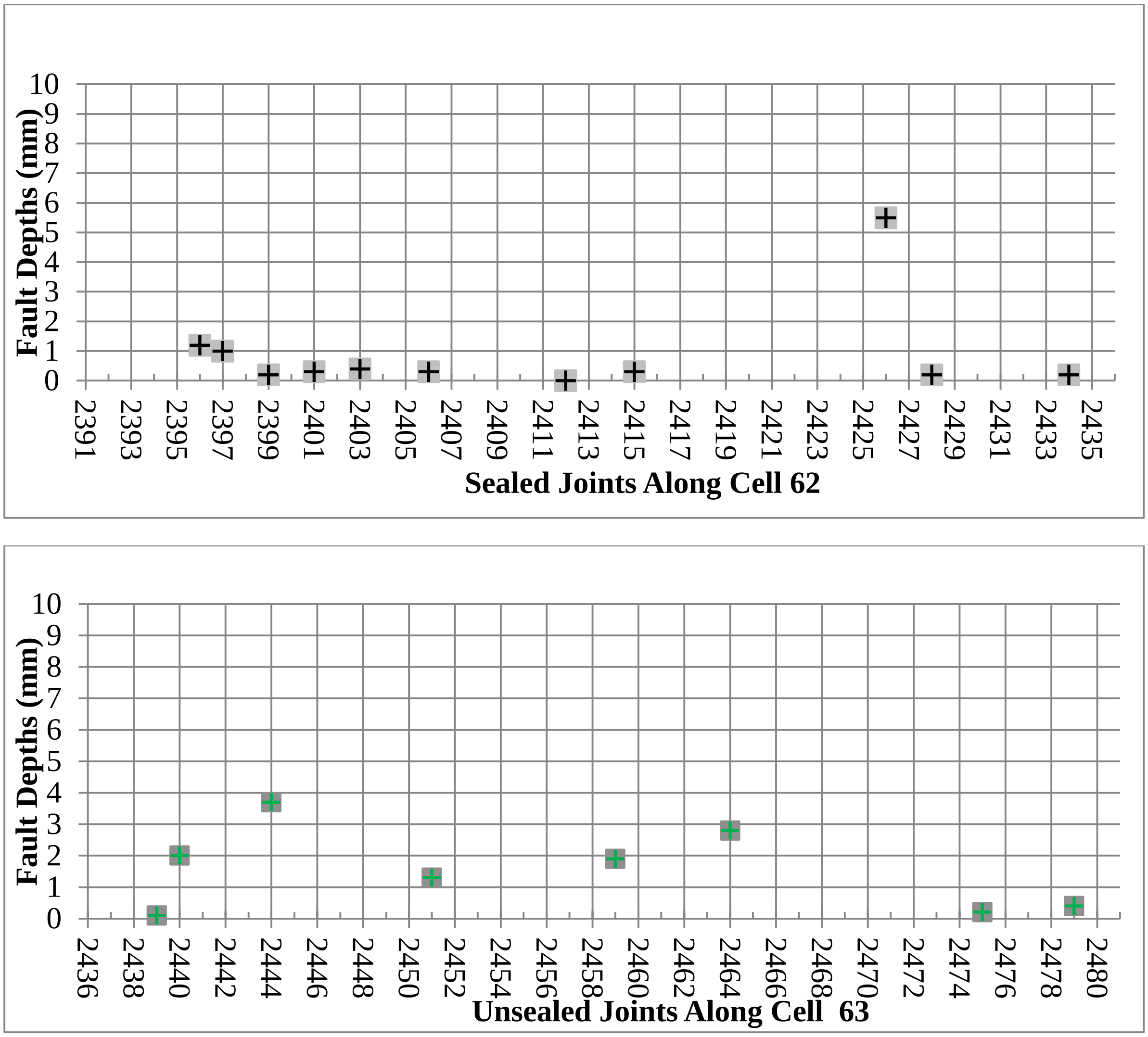

Figure 7 Influence of Joint Sealant on Faulting Development

Effect of Faulting on Roughness

The effect of the magnitude of faulting on pavement roughness is amplified on pavements with smaller panel sizes due to the increased number of transverse joints. With the same magnitude of faulting, a pavement with a longer joint spacing will have a lower International Roughness Index (IRI) than a pavement with a short joint spacing. As previously noted, the designs for Cells 96 and 97 are identical except the panel size. The joint spacing for Cell 96 is 1.5 m (5 ft) while the spacing is 3 m (10 ft) for Cell 97. The IRI for the cells were similar, as can be seen in Figure 8a. However, as can be seen in Figure 8b, the magnitude of faulting for the joints in Cell 97 is higher than the magnitude of the faulting in Cell 96. Therefore, the closer joint spacing produced a similar ride to the longer joint spacing despite having significantly lower faulting. It should be noted that

Cell 96 has not exhibited any cracking and Cell 97 only exhibited mid-slab longitudinal cracking so the only distress contributing to the decrease in IRI for both is faulting. The interesting aspect is that if just the average faulting along the section was evaluated then the performance of Cell 96 and 97 would appear to be the same, as shown in Figure 9. The contribution of the faulting to the increase in IRI can only be found by evaluating the faulting of individual joints. The increase in roughness caused by the additional joints for the shorter slabs when compared to the same magnitude of faulting for longer slabs must be accounted for when establishing faulting failure criteria for BCOAs with short slabs.

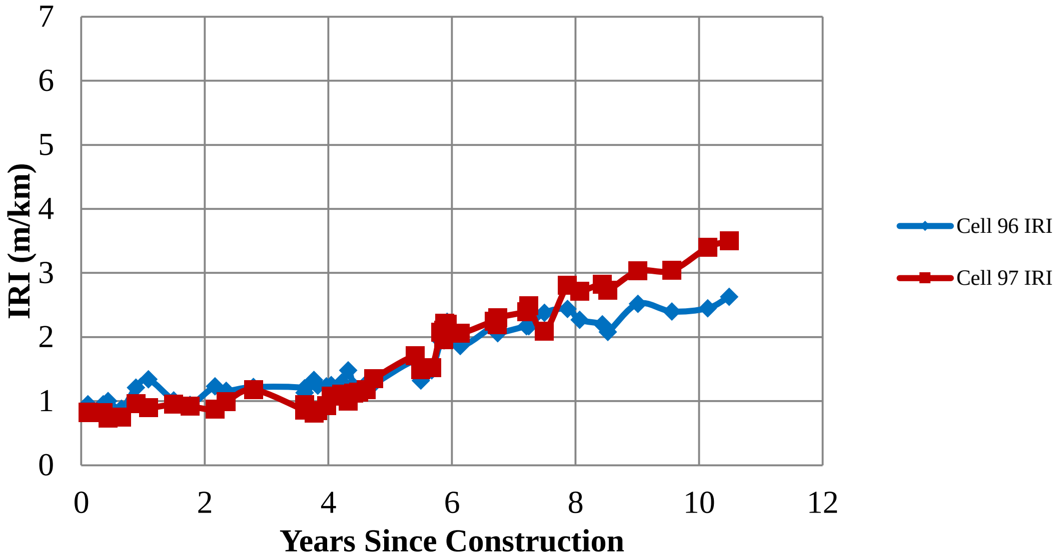

a) IRI for MnROAD Cells 96 and 97

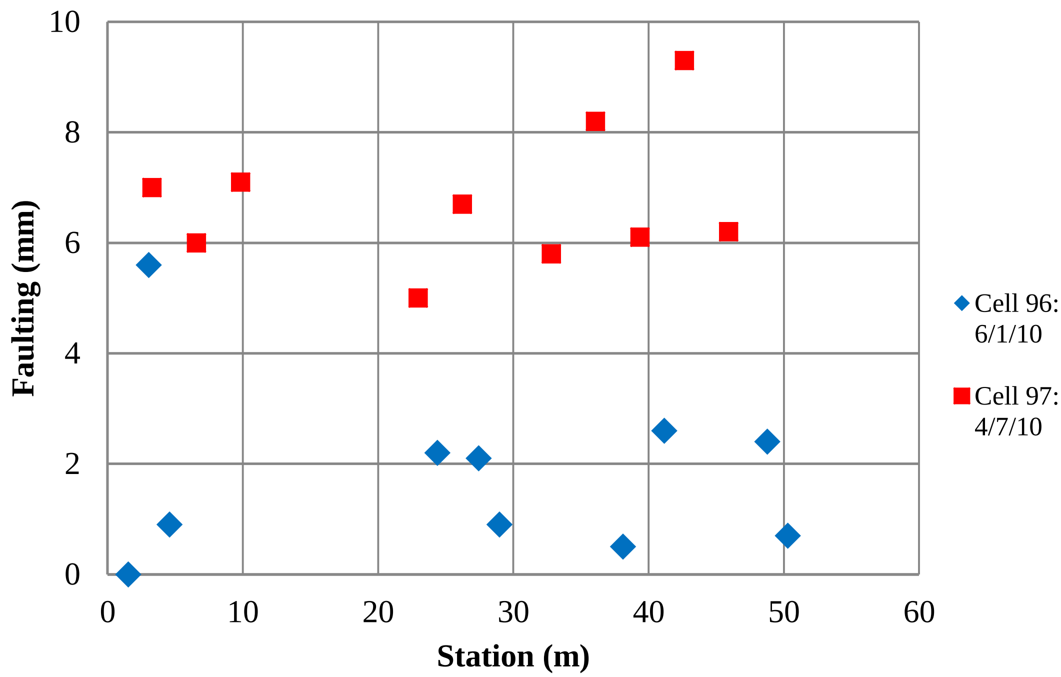

b) Faulting for MnROAD Cells 96 and 97

Figure 8 IRI and Faulting for MnROAD Cells 96 and 97

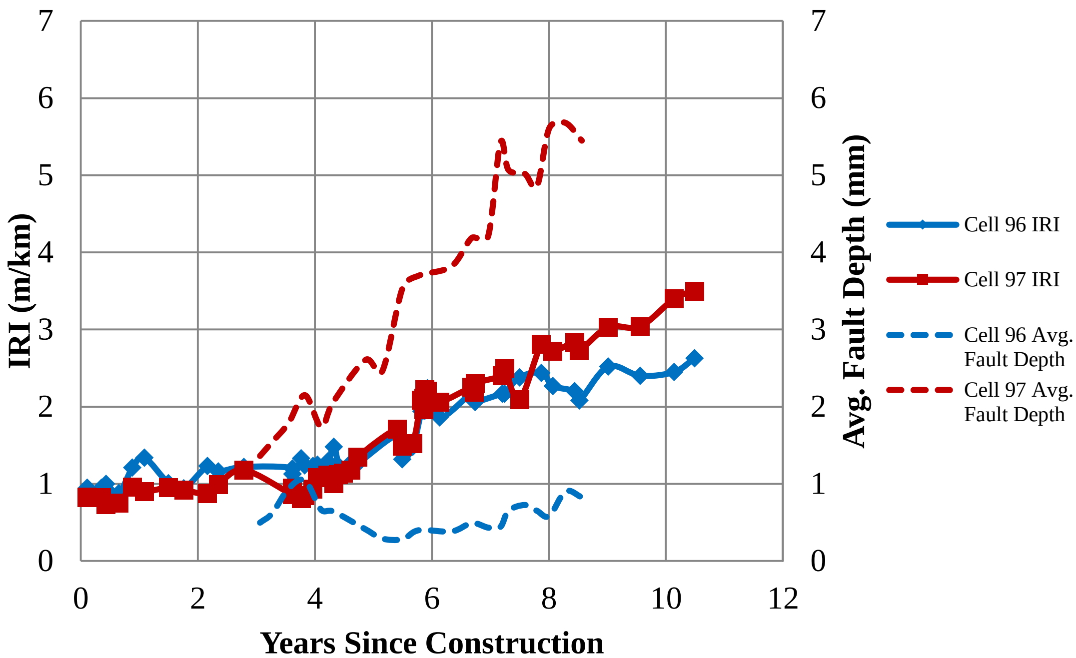

Figure 9 IRI and Average Faulting for MnROAD Cells 96 and 97

Prediction of BCOA Faulting in Pavement ME

The faulting model incorporated into Pavement ME (AASHTO 2008; AASHTO 2011; AASHTO 2012) was developed primarily for JPCP. With this model, faulting starts to develop at a relatively constant rate as soon as the pavement is open to traffic. The faulting rate then decreases with time. Pavement ME also does not predict a dormant period with little to no faulting development early in the service life. In Pavement ME, a BCOA is analyzed as a JPCP on an asphalt base, and pumping is assumed to occur at the PCC/asphalt interface. In actuality, when the joint activates through the asphalt, the pumping occurs in the granular layer beneath the asphalt. The measured and predicted average faulting for Cell 97 can be seen in Figure 10. The erosion resistance of the asphalt is higher than the erosion resistance of the granular layer, which may contribute to the software under predicting faulting in this section.

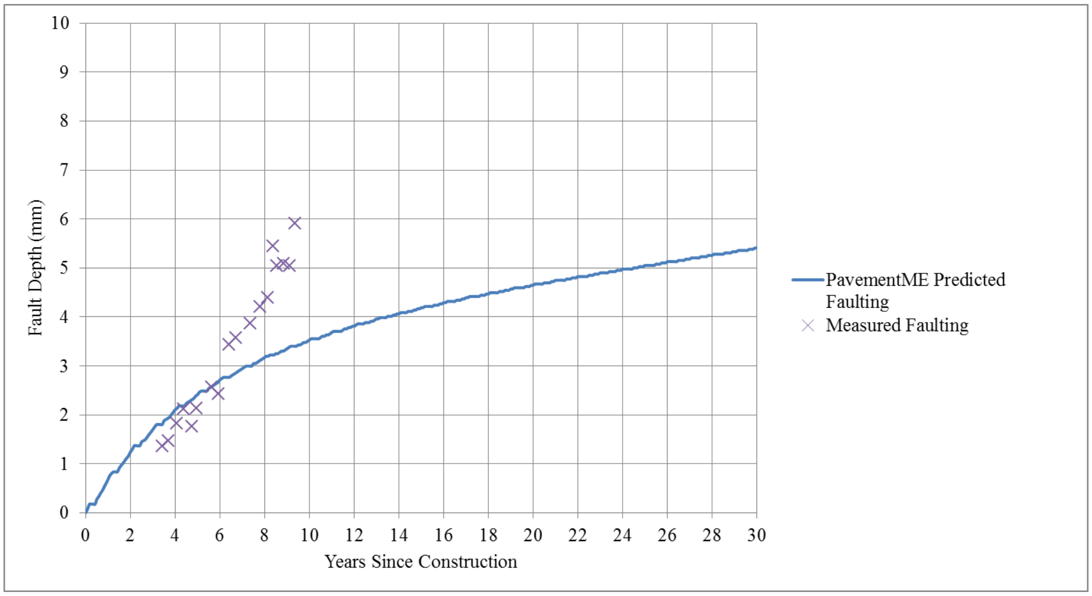

Figure 10 Pavement ME Predicted Faulting for MnROAD Cell 97

Both the predicted and measured faulting experience a gradual increase, however the measured faulting occurs at a faster rate. As mentioned earlier, this may be due to the fact this model represents pumping that develops at the top of the erosion resistant asphalt layer rather than in the more erodible underlying granular layer. The model in the Pavement ME also does not predict the dormant period at the beginning of the service life when minimal to no faulting develops. It is unknown if the faulting development rate would have begun to decrease with time similar to that predicted using the model in the Pavement ME prediction as no additional data is available. In general, if the Pavement ME model is modified to account for the time it takes for a joint to activate through the asphalt and use the erodibility index of the base layer instead of the asphalt layer, it may be useful in predicting the development of faulting in BCOAs when the joints activate through the asphalt. However, it might be more of a challenge for the Pavement ME model to be used to predict faulting in joints that do not activate through the asphalt. Faulting development in these joints could be controlled by the rate of bond deterioration between the PCC and asphalt layers.

Conclusions and Recommendations

Faulting in BCOA can develop from pumping at two separate locations; at the top of asphalt or in the granular material beneath the asphalt. The joint activation can be either through the PCC, through the PCC and asphalt, or not active at all. When the joint does not activate through the asphalt, pumping will occur on the top of the asphalt layer. However, when a joint activates through the asphalt, pumping will occur in the granular layer below the asphalt. The depth the crack propagates at the joint below the pavement surface can be determined using FWD data. The measured LTE at a fully activated joint will be lower than at a joint that has not activated through the asphalt. Field coring provided verification that pumping at the different locations was occurring.

The activation of joints through the asphalt is dictated by several factors. One of the primary factors is the FSR between the PCC layer and the asphalt layer. Pumping of the granular material below the asphalt in the MnROAD cells is unlikely to occur in BCOA sections with a

FSR_{winter} less than or equal to 0.4 because crack activation through the asphalt is unlikely for these pavement structures. BCOA with a FSR_{winter} greater than or equal to 0.9 are likely to develop a crack through the asphalt layer. In addition, the panel size also likely has an effect on the activation of joints through the asphalt. However, panel size is confounded by the FSR at MnROAD, making it difficult to isolate the effect of panel size on joint activation depth. Finally, material properties such as the CTE of the materials, drying shrinkage of the PCC, creep of the asphalt, and fracture properties of the materials will also influence joint activation depth.

Evidence of stained shoulders provides verification that pumping is occurring in these structures whether or not the joint activates through the asphalt. The shape of the faulting development curve depends on whether the joint activates through the asphalt. If the joint activates through the asphalt minimal to no faulting will develop in the first few years, followed by a gradual increase in the development of faulting. If the joint does not activate through the asphalt there is a similar dormant period, followed by a rapid development of faulting. In addition, panel size can influence the joint width and therefore fault development rate. BCOA with larger panels will have a wider joint opening during the colder temperatures, and will develop faulting more rapidly than BCOA with smaller panels. Joint sealant was found to be important to the performance of BCOA when the crack does not activate through the asphalt as well. Water which enters joints that have not activated through the asphalt can become trapped and lead to the rapid development of faulting.

Finally, it was found that the current Pavement ME faulting prediction model might be useful in predicting faulting when pumping is occurring at the top of the granular layer, however adjustments must be made. It will be more challenging to use this model for predicting faulting that occurs due to pumping on top of the asphalt layer at the PCC/asphalt interface.

Acknowledgement

The authors would like to thank the California Department of Transportation for funding this research effort. They would also like to acknowledge Dr. John Harvey for his contributions in this collaborative effort.

References

AASHTO. (2008). Mechanistic-Empirical Pavement Design Guide, Interim Edition: A Manual of Practice. American Association of State Highway and Transportation Officials, Washington, D.C.

AASHTO. (2011). AASHTOWare® DARWin-ME™ v.1.0 Mechanistic-Empirical Pavement Design Software. American Association of State Highway and Transportation Officials, Washington, D.C.

AASHTO. (2012). AASHTOWare Pavement ME Design. American Association of State Highway and Transportation Officials, Washington, D.C.

Burnham, T.R. (2005). "Forensic Investigation Report for Mn/ROAD Ultra-thin Whitetopping Test Cells 93, 94, and 95. Report MN/RC -2005-45.

Burnham, T.R. (2006). "Construction Report For MnROAD Thin Whitetopping Test Cells 60-63." Report MN/RC – 2006-18.

http://dotapp7.dot.state.mn.us/research/dataproduct/Data%20Release/ (April 1, 2015).

Li, Z., and Vandenbossche, J.M., (2013). "Redefining the Failure Mode for Thin and Ultra-thin Whitetopping with a 1.8-x1.8-m (6-x6-ft) Joint Spacing." Transportation Research Record: Journal of the Transportation Research Board, No. 2368, pp. 133-146.

Mack, J. W., Cole, L. W., and Mohsen, J. P. (1993). "Analytical Considerations for Thin Concrete Overlays on Asphalt." Transportation Research Record: Journal of the Transportation Research Board, No. 1388, pp. 167–173.

Mack, J. W., Hawbaker, L. D., and Cole, L. W. (1998). "Ultrathin Whitetopping: State-of-the-Practice for Thin Concrete Overlays of Asphalt." Transportation Research Record: Journal of the Transportation Research Board, No. 1610, pp. 39–43.

Rasmussen, R.O., McCullough, B.F., Ruiz, J.M., Mack, J., and Sherwood, J.A. (2002). "Identification of Pavement Failure Mechanisms at FHWA Accelerated Loading Facility Ultrathin Whitetopping Project." Transportation Research Record: Journal of the Transportation Research Board, No. 1816, pp. 148-155.

Mu F., and Vandenbossche, J.M. (2011). "Development of a Rational of Mechanistic- 44 Empirical Based Design Guide for Thin and Ultra-Thin Whitetopping. Task 2 Report: Review and Selection of Structural Response Models." University of Pittsburgh. February 2011.

Roesler, J., Bordelon, A., Ioannides, A., Beyer, M., and Wang, D. (2008). "Design and Concrete Material Requirements for Ultra-Thin Whitetopping." Federal Highway Administration, Report No. FHWA-ICT-08-016, Illinois Center for Transportation, Illinois.

Vandenbossche, J. M., and Barman, M. (2010). “Bonded Whitetopping Overlay Design Considerations for Prevention of Reflection Cracking, Joint Sealing, and the Use of Dowel Bars.” Transportation Research Record: Journal of the Transportation Research Board, No.2155, pp. 3-11.

Vandenbossche, J. M. and Fagerness, A. J. (2002). “Performance, Analysis, and Repair of Ultrathin and Thin Whitetopping at Minnesota Road Research Facility.” Transportation Research Record: Journal of the Transportation Research Board, No. 1809, pp. 191-198.

Vandenbossche, J. M. and Rettner, D. L. (1998). “The Construction of US-169 and I-94 Experimental Thin and Ultra-Thin Whitetopping Sections in Minnesota.” Report MN/RC -2001-07.

Wu, C. L., Tarr, S. M., Refai, T. M., Nagi, M. A., and Sheehan, M. J. (1998). “Development of Ultrathin Whitetopping Design Procedure.” Research and Development Series No. 2124. Portland Cement Association, Skokie, Illinois.